Liquid Crystals
Publication details, including instructions for authors and subscription information:
http://www.informaworld.com/smpp/title~content=t713926090

Comparisons of the vector method and tensor method for simulating liquid crystal devices

J. E. Anderson[a]; P. Watson[a]; P. J. Bos[a]
[a] Liquid Crystal Institute and Chemical Physics Interdisciplinary Program, Kent State University, Kent OH 44242, USA,

Online publication date: 06 August 2010

To cite this Article Anderson, J. E. , Watson, P. and Bos, P. J.(2001) 'Comparisons of the vector method and tensor method for simulating liquid crystal devices', Liquid Crystals, 28: 1, 109 — 115
To link to this Article: DOI: 10.1080/02678290010001455
URL: http://dx.doi.org/10.1080/02678290010001455

LIQUID CRYSTALS, 2001, VOL. 28, NO. 1, 109–115

Comparisons of the vector method and tensor method for simulating liquid crystal devices

J. E. ANDERSON*, P. WATSON, and P. J. BOS
Liquid Crystal Institute and Chemical Physics Interdisciplinary Program,
Kent State University, Kent OH 44242, USA

(*Received 24 April 2000; accepted 25 July 2000*)

In calculating the director configuration in a liquid crystal device, two methods are commonly employed: a vector model and a tensor model. In this paper, we compare and contrast these methods for liquid crystal devices consisting of a layer of liquid crystal sandwiched between two plates. We compare the reliability and accuracy of the results, the speed of computation and the complexity of implementations of each method.

1. Introduction

Mathematical simulations provide a powerful tool for the understanding and optimization of liquid crystal displays (LCDs). Usually these simulations are made with a one-dimensional constraint on the change of the director, **n** [1, 2]. However, if a truly accurate model is desired, the simulations must be performed allowing the director to move in two or three dimensions [3–5]. Some LCD modes, such as in-plane-switching (IPS), multi-domain-vertical-alignment (MVA), electro-optic-compensation (EOC), and any multi-domain configuration, must use these more advanced simulation techniques, since they are designed to use a multi-dimensional effect, and cannot therefore be approximated by a one-dimensional simulation. These more advanced simulations take more computing time, and it is necessary to know that the results can be trusted and that the program is optimized to run as fast as possible. It is the aim of this paper to establish, in terms of the mathematical model, how to achieve these requirements.

2. Inversion symmetry

In experiment, one cannot discern an absolute direction of the director. This is because, on average, half of the molecules are pointing in the opposite direction to the other half. This is shown schematically in figure 1.

This symmetry is typically called 'inversion symmetry' or 'the **n** and $-\mathbf{n}$ equivalence'. Because this **n** and $-\mathbf{n}$ equivalence of the free energy found in experiment is retained in the tensor approach, it has generally been assumed to be superior to the vector approach, in which this equivalence is not kept [6–8]. Kelly originally pointed out that the tensor approach did not give correct answers for some two-dimensional simulations [9]. We have also found cases in which the tensor approach gave not only inaccurate results, but non-physical results. In each of these cases, the tensor approach allowed the system to transform between topologically inequivalent states without a disclination, which is impossible in reality [10, 11]. Although we use only one form of the tensor approach here [6, 7], this problem is suspected to exist in all forms, as it is a fundamental aspect of a mathematical tensor.

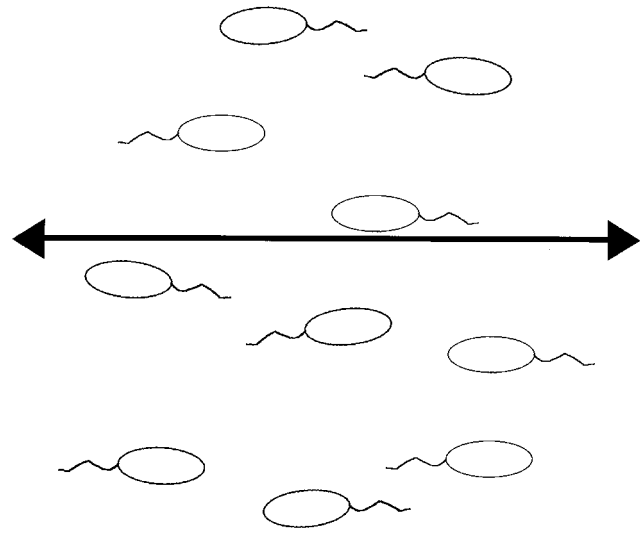

Figure 1. Schematic drawing of the nematic liquid crystal phase showing that the director cannot be said to point to either the right or left. The arrow shows the average direction of alignment, which is the director.

* Author for correspondence; e-mail: janderson@hanach.com

Liquid Crystals ISSN 0267-8292 print/ISSN 1366-5855 online © 2001 Taylor & Francis Ltd
http://www.tandf.co.uk/journals
DOI: 10.1080/02678290010001455

3. Mathematical models

There are many approaches to the simulation of LCDs. The simplest method uses two angles to represent the director: θ, the polar angle measured from the surface normal, and ϕ, the azimuthal angle (the $\theta - \phi$ approach) [1]. The Oseen–Frank free energy density, equation (1), is written in terms of these variables, as given in equation (2).

$$f = \frac{1}{2}K_{11}(\nabla \quad \mathbf{n})^2 + \frac{1}{2}K_{22}(\mathbf{n} \quad \nabla \times \mathbf{n} + q_0)^2 + \frac{1}{2}K_{33}|(\mathbf{n} \times \nabla \times \mathbf{n})|^2 - \frac{1}{2}\mathbf{D} \quad \mathbf{E} \tag{1}$$

$$f = \frac{1}{2}K_{11}\sin^2\theta\left(\frac{\mathrm{d}\theta}{\mathrm{d}z}\right)^2 + \frac{1}{2}K_{22}\left[\sin^4\theta\left(\frac{\mathrm{d}\phi}{\mathrm{d}z}\right)^2 + 2q_0\sin^2\theta\left(\frac{\mathrm{d}\phi}{\mathrm{d}z}\right) + q_0^2\right] + \frac{1}{2}K_{33}\left[\cos^2\theta\left(\frac{\mathrm{d}\theta}{\mathrm{d}z}\right)^2 + \sin^2\theta\cos^2\theta\left(\frac{\mathrm{d}\phi}{\mathrm{d}z}\right)^2\right] - \frac{1}{2}\mathbf{D} \quad \mathbf{E}. \tag{2}$$

In this representation, if θ becomes close to zero (the homeotropic state), the free energy becomes almost independent of ϕ, as the azimuthal angle is undefined when the director is homeotropic. This leads to mathematical instabilities in simulation, and therefore this approach is rarely used. The next approach is to use the cartesian coordinate vector, $\mathbf{n} = (n_x, n_y, n_z)$ (the vector approach). Writing the free energy in this way removes any mathematical instability when any director in the system is close to homeotropic.

To calculate director dynamics, the viscous torque is set equal to the elastic torque, in equation (3), where γ_1 is the rotational viscosity [1–7]. This can then be discretized to find the new value of the director. This new director then needs to be renormalized to be of unit length [7].

$$\gamma_1\frac{\mathrm{d}n_i}{\mathrm{d}t} = -\frac{\delta f}{\delta n_i} \Rightarrow \gamma_1\frac{\Delta n_i}{\Delta t} = -\frac{\delta f}{\delta n_i} \Rightarrow n_i^{\mathrm{new}} = n_i^{\mathrm{old}} - \frac{\Delta t}{\gamma_1}\frac{\delta f^{\mathrm{old}}}{\delta n_i} \tag{3}$$

where in three dimensions:

$$\frac{\delta f}{\delta \xi} = \frac{\partial f}{\partial \xi} - \frac{\mathrm{d}}{\mathrm{d}x}\left[\frac{\partial f}{\partial(\mathrm{d}\xi/\mathrm{d}x)}\right] - \frac{\mathrm{d}}{\mathrm{d}y}\left[\frac{\partial f}{\partial(\mathrm{d}\xi/\mathrm{d}y)}\right] - \frac{\mathrm{d}}{\mathrm{d}z}\left[\frac{\partial f}{\partial(\mathrm{d}\xi/\mathrm{d}z)}\right] \tag{4}$$

where ξ is the variable whose dynamics are desired.

As stated above, the nematic phase is partially characterized by the fact that the free energy is invariant under the transformation $\mathbf{n} \rightarrow -\mathbf{n}$. This equivalence is not maintained in the vector approach, as shown by several authors [5–8]. To correct this, the free energy is often written in terms of the order parameter tensor given in equation (5).

$$Q_{jk} = S(n_j n_k - \delta_{jk}/3). \tag{5}$$

Here $j, k = x, y, z$, δ_{jk} is equal to 1 if $j = k$ and 0 otherwise, and S is the scalar order parameter. The diad, $(n_j n_k)$, in the order parameter tensor in effect squares the director components, thus restoring the inversion symmetry found in experiment.

The free energy written in terms of this tensor is given in equation (6) [12]. The $G_i^{(j)}$ terms are 'de Gennes strain terms'. Note that the last two terms in equation (6) are electric energy terms. This will hereafter be referred to as the tensor approach.

$$f = \left(\frac{-K_{11}}{12} + \frac{K_{22}}{4} + \frac{K_{33}}{12}\right)\frac{G_1^{(2)}}{S^2} + \left(\frac{K_{11} - K_{22} - K_{24}}{2}\right)\frac{G_2^{(2)}}{S^2} + \frac{K_{24}}{2}\frac{G_3^{(2)}}{S^2} + \left(\frac{K_{33} - K_{11}}{4}\right)\frac{G_6^{(3)}}{S^3} = q_0 K_{22}\frac{G_4^{(2)}}{S^2} - \frac{1}{2}\varepsilon_0\langle\varepsilon\rangle\frac{\mathrm{d}V}{\mathrm{d}j}\frac{\mathrm{d}V}{\mathrm{d}j} - \frac{1}{2}\varepsilon_0\Delta\varepsilon\frac{\mathrm{d}V}{\mathrm{d}j}\frac{\mathrm{d}V}{\mathrm{d}k}\frac{Q_{jk}}{S} \tag{6}$$

where:

$$G_1^{(2)} = Q_{jk,l}Q_{jk,l}, \quad G_2^{(2)} = Q_{jk,k}Q_{jl,l}, \quad G_3^{(2)} = Q_{jk,l}Q_{jl,k}, \quad G_4^{(2)} = e_{jkl}Q_{jm}Q_{km,l}, \quad G_6^{(3)} = Q_{jk}Q_{lm,j}Q_{lm,k} \tag{7}$$

To calculate the new value of the director using the tensor approach, the functional derivatives need to be taken with respect to Q_{jk}, instead of n_i. This can be done using the chain rule, equation (8) [7]:

$$\frac{\delta f}{\delta n_i} = \frac{\delta f}{\delta Q_{jk}}\frac{\partial Q_{jk}}{\partial n_i}, \quad \frac{\partial Q_{jk}}{\partial n_i} = S(n_j\delta_{ki} + n_k\delta_{ji}). \tag{8}$$

Here summation over repeated indices is assumed. When the functional derivative of f with respect to Q_{jk} is taken, the derivative pulls past the elastic constants (K_{ii}) and is taken on the de Gennes strain terms.

If a system contains defects with strength $N \times (1/2)$ where N is any odd integer, the vector approach, because it lacks inversion symmetry will not calculate the energy correctly. However, in cases where such defects exist, one of the basic assumptions of continuum theory, that changes in the director are on length scales much larger

than a molecular length and the system is therefore continuous, breaks down, and continuum theory itself is mathematically insufficient.

4. Topologically equivalent and inequivalent states

As pointed out by Porte [10] and Thurston [11], every director configuration cannot be continuously transformed to every other director configuration. There are certain sets of configurations that can be continuously transformed between each other within the set, but cannot be continuously transformed to a configuration in another set. A director configuration is said to transform continuously to another configuration if no defect is involved.

To illustrate topological equivalence and inequivalence, we will use the Bistable Twist Cell device. The three states that can be found in this device are shown in figure 2. This device uses the fact that the 0 degree twist state and the 360 degree twist state are topologically equivalent. By using the correct driving waveform, each pixel can be made to be in either state. To ensure that both the 0 degree twist state and the 360 degree twist state can be formed in these devices, a chiral dopant is added such that both states are (or nearly are) of equal energies. This usually makes the third state, the 180 degree twist state, the lowest free energy. Figures 2(*a*) and 2(*c*) show the 0 degree twist and 360 degree twist states, respectively. If the surface contacting director on the bottom surface is described by (θ_p, ϕ_p), the same value describes the surface contacting director on the top surface for the 0 degree and 360 degree twist states. However, for the 180 degree twist state, the surface contacting director on the top surface is given by $(180 - \theta_p, \phi_p + 180)$.

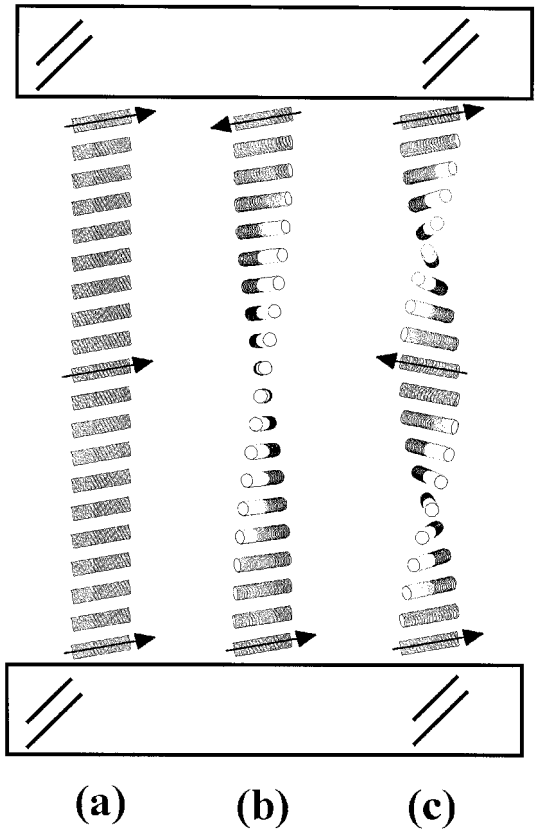

Figure 2. The three possible states in a Bistable Twist Cell: (*a*) 0 degree twist state, (*b*) the undesired 180 degree twist state, and (*c*) 360 degree twist state. Note that the 0 degree and the 360 degree twist states have the same vector boundary conditions. The 180 degree twist state, however, has one boundary condition pointing in the opposite direction. The director configurations were drawn using LC3Draw visualization software.

For example, point A on the sphere shown in figure 3 represents one boundary condition, namely $\theta = 80$ degrees and $\phi = 0$ degrees. For the 0 degree state and the 360 degree state, point A represents the director at both boundaries, as pointed out above. The 360 degree twist configuration is also shown in figure 3. The 360 degree twist state is said to be topologically equivalent to the 0 degree twist state because the representation on the unit sphere of the 360 degree state can be continuously transformed to the 0 degree state. The 0 degree state is a uniform structure, and so the entire configuration is represented by the point A. Point A′ represents the $\theta = 100$ degrees and $\phi = 180$ degrees boundary condition needed for the top surface in the 180 degree state.

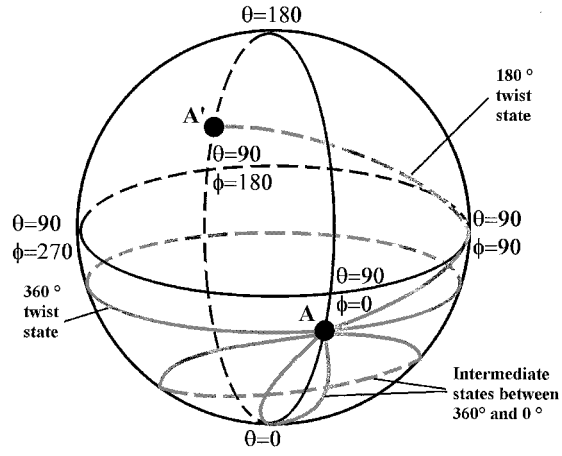

Figure 3. Unit sphere representation of topologically equivalent and inequivalent states. The **n** and − **n** equivalence of the nematic phase causes the diametrically opposed points, A and A′, to be the same physical boundary condition. It is clear that the 360 degree and 0 degree states (entirely represented by point A), are topologically equivalent, because they can be continuously transformed from one to the other. The 180 degree state, however, because one of its boundary conditions is represented by point A′, is topologically inequivalent to either the 360 degree or 0 degree states.

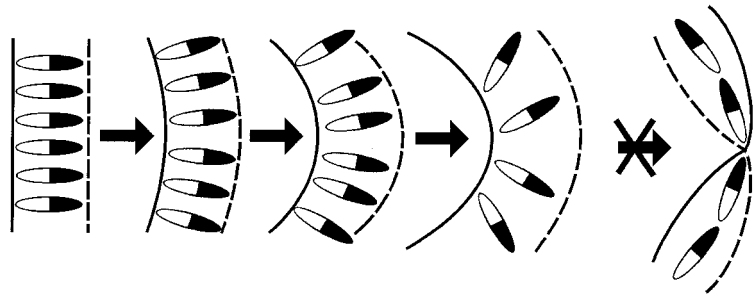

Figure 4. Stretching of a uniform state into a splay state. No amount of stretching will ever cause the deformation to become a bend deformation, shown on the right. The lines denote the continuous nature of the nematic phase.

The inversion symmetry found in experiment tells us that points A and A′, which are diametrically opposite on the sphere, are *exactly* the same physical boundary condition. That is to say, there is no way in experiment to differentiate between the two. However, it is clear that there is no way to transform the 180 degree twist state to either the 360 degree state or the 0 degree state without 'moving' the boundary condition at A′ to lie at point A. Therefore, within the realm of the Frank–Oseen description of the director field, it is impossible to transform between the 180 degree twist state and the 0 degree or 360 degree twist states.

The physical reason that topologically distinct states exist is that liquid crystal systems are continuous, not discretized as we think of them in simulation. If a uniformly aligned configuration is stretched, as shown in figure 4, it forms a typical splay state. No matter how much we try to stretch it, it can never be made to go into the bend state in a continuous manner. A disclination, which is outside the scope of the Frank–Oseen description, is required to move across the sample for this transition to occur.

We will now investigate the two mathematical models, the vector model and the tensor model, to determine whether either allows a non-physical continuous transition between topologically inequivalent states.

5. Simulations

Although the equivalence of **n** and $-\mathbf{n}$ exists in the nematic phase, we will show here that, because a discretized system is used in simulations, care should be taken when such symmetry exists in programs. The concern of including this equivalence in simulations of liquid crystal devices is that it can lead to non-physical results when a director deformation falls completely between two adjacent grid points, as can be considered to happen when the angle between the directors of two adjacent grid points is greater than 90 degrees. If a deformation does slip completely between two adjacent grid points, the grid is obviously too coarse and a finer grid should be used. However, we seldom know before we start the calculation how many grid points should be used. It is possible with the tensor approach, as we will show, for a deformation to slip between adjacent grid points during the computation and for the simulation to show inaccurately a transition between topologically distinct states. This is especially true for more complicated systems, such as highly twisted cholesterics.

Figures 5, 6 and 7 present three cases where the tensor approach incorrectly shows continuous transitions between topologically inequivalent states. In all figures, (*a*) refers to the configurations calculated by the vector method, and (*b*) refers to the configurations calculated by the tensor method. We used the physical parameters of ZLI 4792 from Merck in all simulations. The cell thickness was assumed to be 5 μm and in each case the applied field, whether it be an electric field caused by applying 10 V, or a magnetic field, was turned on at 0 ms and off at 60 ms.

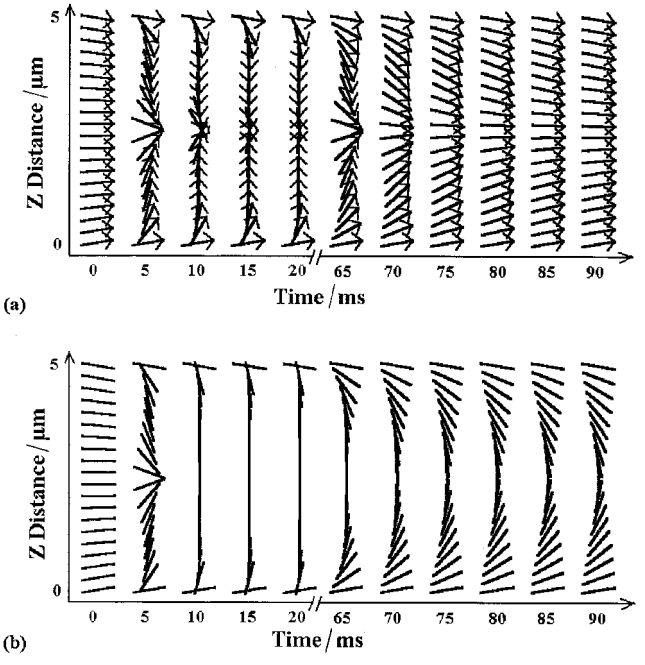

Figure 5. Dynamics of pi-cell with 10 V applied. Voltage was turned on at 0 ms, and removed at 60 ms: (*a*) used the vector approach and (*b*) used the tensor approach. The tensor approach clearly shows a continuous transition from the splay state to the bend state, which is impossible in experiment.

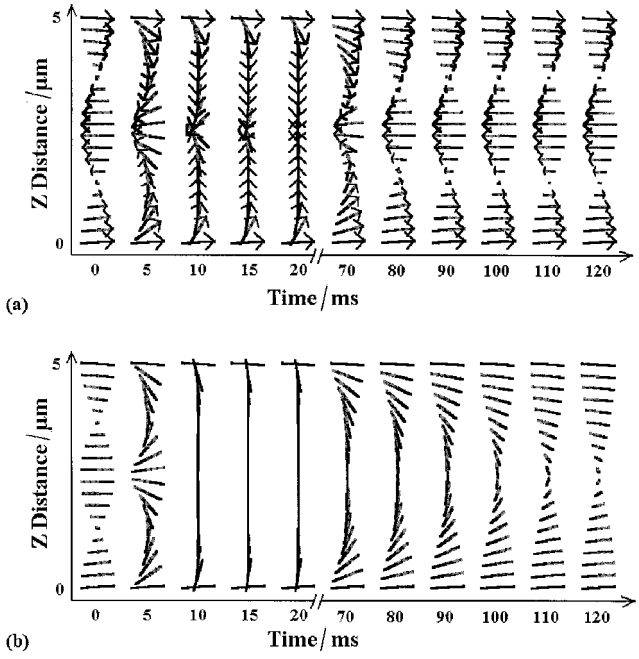

Figure 6. Dynamics of 360 degree STN with d/P of 1.0 and 10 V applied. The voltage was turned on at 0 ms and removed at 60 ms: (*a*) used the vector approach and (*b*) used the tensor approach. The tensor approach again clearly shows a continuous transition between two topologically distinct states, the 360 degree and the 180 degree twist states. The light gray parts of the director are away from the viewer.

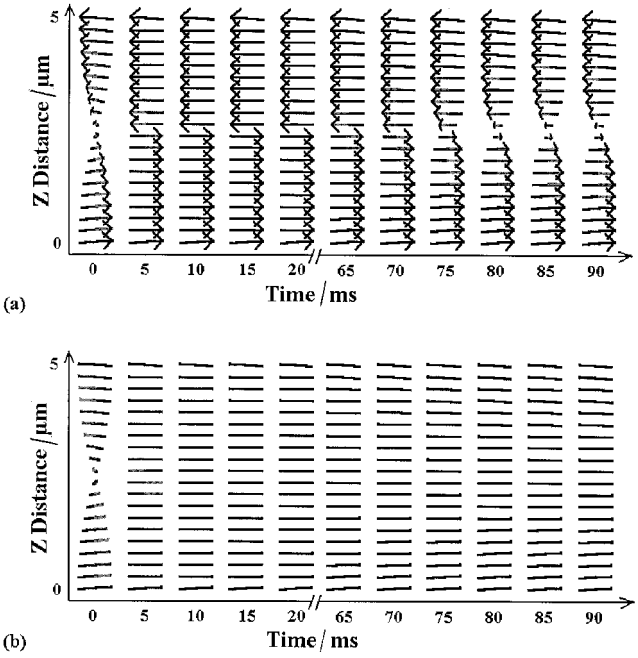

Figure 7. Dynamics of a 180 degree STN with a d/P of 0.3 and a lateral magnetic field applied. The magnetic field was turned on at 0 ms and removed at 60 ms: (*a*) used the vector approach and (*b*) used the tensor approach. The tensor approach clearly shows a continuous transition from the 180 degree twist state to the almost uniformly aligned splay state. The light gray parts of the director are away from the viewer.

We calculated the dynamic director configuration as a function of time for a pi-cell with pretilts of 10 degrees using both methods, as shown in figure 5. We started the system in the splay state and applied 10 V at time $t = 0$. The voltage was applied for 60 ms, which was long enough for both simulation methods to show the centre region to be homeotropic. When the field was switched off, however, the simulation using the vector approach showed the system return to the splay configuration, while the simulation using the tensor approach showed a continuous transformation to the bend state. In an actual sample, these two states are topologically inequivalent and therefore cannot be transformed from one to the other without the movement of a defect. It can be seen that, at $t = 60$ ms, the region of splay fits entirely between two adjacent grid points. That is, the two directors in the middle of the cell became completely homeotropically aligned. In the case of the vector model, this leads to a high free energy density because the directors at grid points on either side of the 'invisible' wall point in opposite directions. However, in the tensor approach, when the splay region slips between two adjacent grid points, the $\mathbf{n}$ and $-\mathbf{n}$ equivalence yields a (low free energy) uniform homeotropic director configuration, thus 'losing' the director deformation. The vector approach therefore gives an inexact high value of the elastic free energy density, but yields a more physically correct result than the low elastic free energy density given by the tensor model.

The results of dynamics calculations of a 360 degree super-twisted-nematic (STN) with 10 V applied at $t = 0$ ms and removed at $t = 60$ ms is shown in figure 6. The system had a thickness to pitch ratio (d/P) of 1.0, making the 360 degree twist state the lowest energy state. The alignment in this case was a splayed alignment with 5 degree pretilts. If a non-splayed alignment was used, the material would switch from the 360 degree twist state to the 0 degree twist state, which are topologically equivalent, and of no interest to this investigation. Again, a voltage of 10 V was high enough and was held for a long enough time for the directors in the centre of the cell to become homeotropically aligned. Upon removal of the field, however, the tensor approach showed the system transforming from a 360 degree twist state to a 180 degree twist state, two topologically inequivalent states.

The third simulation used a 180 degree STN having a d/P of 0.3 with a lateral magnetic field applied, the results of which are shown in figure 7. The magnetic field was assumed to be in the x-direction. In this case,

the centre directors are not homeotropically aligned, but homogeneously aligned. The vector method again calculated a high free energy density in the middle of the cell, caused by the two adjacent directors pointing in opposite directions, while the tensor method, because of the **n** and $-$ **n** equivalent, did not. This low free energy density caused the tensor method to transform the system continuously to the topologically distinct (and higher free energy) almost uniform splay state. Figure 8 shows a close up of layers in the middle of the cell in figure 7. This demonstrates the problem with the tensor approach when a deformation (a pi-wall in this case) slips completely between two adjacent grid points. The **n** and $-$ **n** equivalence causes the tensor approach to 'lose' the deformation.

The simulations shown here use an even number of lattice points, thus not putting one directly in the centre of the cell. When an odd number was used, we found that the symmetry point of the deformation was pushed between grid points (probably due to small numerical fluctuations) and the tensor approach still switched topologically distinct states.

One may argue that using a larger number of grid points would correct this non-physical result. However, we found that it only causes the transition between topologically inequivalent states to happen at larger applied fields, not to stop happening completely. When a larger number of grid points (> 50) was used, both approaches gave the correct answer with 10 V applied. However, for each grid spacing tried, we found there was always a voltage (which depended on grid spacing) high enough to force the deformation to fit completely between two adjacent grid points and the tensor approach would again change topological states. This voltage was never greater than 75 V, even at grid spacings down to 25 nm. As stated before, the correct number of grid points to use is not always known before the calculation is started, and the tensor method may not alert the researcher to the fact that a deformation has slipped between grid points, whereas the vector method always will.

To compare the accuracy of the two methods, we calculated the RMS error in the calculations as a function of grid size. To calculate this error, we used an untwisted electrically controlled birefringence (ECB) device system with 3 V applied. Figure 9 shows the RMS error as a function of grid size for both simulation methods. The computed solution using 100 grid points was assumed to be the correct solution, as the director configuration was almost independent of grid size when that many points were used. It can be clearly seen that the vector method always maintains a lower RMS error than the tensor method. The lines are exponential fits shown only to clarify the data.

The vector approach is also a simple method to implement, coming straight from the Frank–Oseen free energy equation. To calculate the functional derivatives of the free energy density with respect to the director components, needed for the update formula given in equation (4) for the tensor approach, we must first calculate the functional derivatives of the free energy density with respect to the components of the order parameter tensor. This is due to the chain rule as shown in equation (8). This adds an extra subroutine that must be implemented in code, and called nine times for each iteration step.

Also, we have found, probably due in large part to the relative simplicity of the vector method, that it is computationally faster. For our implementations, the

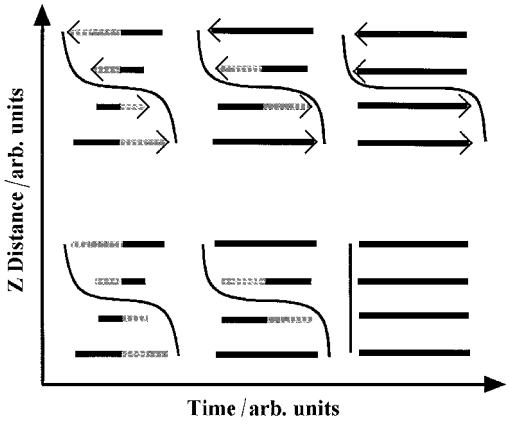

Figure 8. Close up of dynamics of the layers in the middle of the cell in figure 7, showing the tensor method 'losing' the pi-wall between lattice points because of the **n** and $-$ **n** equivalence. The lines illustrate the director distribution assumed by each energy model. The light gray parts of the director are away from the viewer.

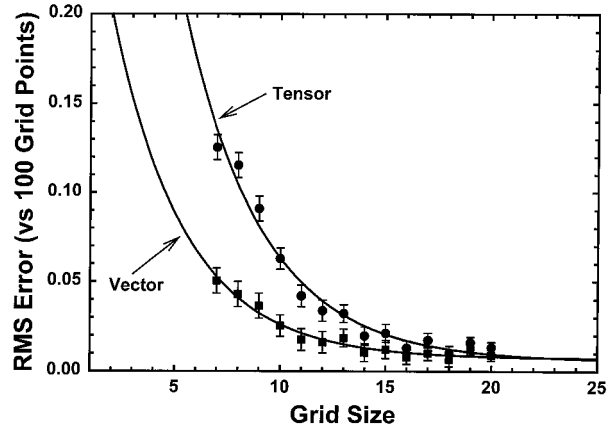

Figure 9. Calculated RMS Error as a function of grid size for the tensor and vector methods. The lines are exponential fits shown to clarify the data. The solution using 100 grid points was assumed to be the exact solution.

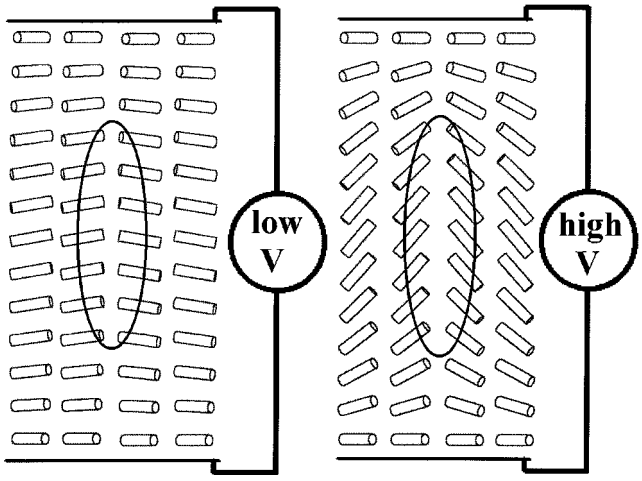

Figure 10. 2-D cartoon of reverse-tilt domain in a 90 degree TN. At low voltages, both the vector and tensor methods will calculate bend energy across the wall. At higher voltages, however, the tensor method will calculate the energy to be splay energy, which will yield incorrect results. As shown in figure 3, no amount of 'stretching' should make the deformation switch from bend to splay.

vector approach was roughly 1.3 times faster for one-dimensional calculations and 3 times faster for two- and three-dimensional calculations. Although these numbers will obviously depend on the exact implementation, the vector method, due to its simpler coding, will always run faster. The vector method is also easier to optimize, as the code is easier to handle.

In this report, we have only shown calculated results for one-dimensional simulations because it is possible to know what the physical results must be for these reduced cases. However, all the conclusions must be the same for multi-dimensional cases as well, because all that is needed for the tensor approach to give a non-physical result is for a deformation to fall completely between two adjacent grid points. This can happen in any direction, not just the z-direction. A conceptual case is shown in figure 10.

On the left side of figure 10, when a 90 degree TN has low voltage applied, a reverse tilt domain has bend energy across the wall. This energy should remain bend energy, by the continuity of the director field, as we have shown in figure 3. However, when the voltage is increased, the discretization causes the angle between the directors to increase and thus the tensor model would calculate a splay free energy across the wall. This will yield incorrect results when investigating the reverse-tilt domain and how to remove it from a device.

6. Conclusion

Because the **n** and $-$ **n** equivalence of the free energy found in experiment is retained in the tensor approach to simulations, it has been assumed to be superior to the vector approach, which it is not. We have shown three cases where the **n** and $-$ **n** equivalence causes the tensor method to give non-physical results. The vector approach is also found to be faster and require fewer grid points than the tensor method.

Funding for this project was provided by DAFPA grant No. N61331-96-C-0042 and was performed in an institute funded by ALCOM grant No. DMR-8920147-09. Some figures were reproduced with permission from reference [13].

References

[1] Berreman, D. W., 1974, *Appl. Phys. Lett.*, **25,** 12.
[2] Berreman, D. W., 1982, *Phil. Trans. R. Soc. Lond. A*, **309,** 203–216.
[3] Lien, A., and Chen, C.-J., 1996, *SID Dig. Tech. Pap.*, **27,** 175.
[4] Lien, A., 1993, *Appl. Phys. Lett.*, **62,** 1079.
[5] Haas, G., Siebert, S., and Mlynski, D. A., 1989, *Jpn. Disp. Dig.*, 524.
[6] Killian, A., and Hess, S., 1989, *Z. Naturforsch.*, **A44,** 693.
[7] Dickmann, S., 1993, PhD thesis, U. Karlsruhe, Germany.
[8] Haas, G., Wöhler, H., Fritsch, M. W., and Mlynski, D. A., 1990, *Proc. SID*, **31,** 301.
[9] Kelly, J., 1998, *SID 98*, 21.3.
[10] Porte, G., 1977, *J. de Phys.*, **38,** 509.
[11] Thurston, R. N., 1981, *J. appl. Phys.*, **52,** 3040.
[12] Dickmann, S., Eschler, J., Cossalter, O., and Mlynski, D. A., 1993, *SID Dig. Tech. Pap.*, **24,** 638.
[13] Anderson, J. E., Watson, P., and Bos, P. J., 1999, *SID Dig. Tech. Pap.*, **30,** 198.